J Mater Sci (2015) 50:2577–2586
DOI 10.1007/s10853-015-8823-5

Enhanced photocatalytic activity of TiO_2@mercapto-functionalized silica toward colored organic dyes

Hwan Hui Yun · Jung Soo Kim · Euk Hyun Kim · Sang Kyoung Lee · Jin Woo Kim · Hyung Jun Lim · Sang Man Koo

Received: 2 September 2014 / Accepted: 30 December 2014 / Published online: 21 January 2015

Abstract Core–shell-type TiO_2@mercaptopropyl-functionalized silica (MPS) particles were prepared for enhanced photocatalytic performance of TiO_2. The MPS particles were adopted in the composite-type photocatalyst design so as to enhance the photo-catalytic activity through the chemical interaction between chemically modified substrate particles and organic dye molecules, although they do not have photocatalytic activity. Three organic dyes, rhodamine B, rhodamine 6G, and methyl orange, were selected for testing dye adsorption characteristics and photocatalytic activities of the TiO_2@MPS particles, commercial P25, and unsupported TiO_2 nanosols. Rhodamine B and rhodamine 6G dyes were adsorbed much more on the TiO_2@MPS particles than P25, by factors of 6 and 43, respectively, while methyl orange molecules were adsorbed more readily on P25. Such difference in the dye adsorption characteristics of the two photocatalysts may be related with available functional groups and the dyes. This would lead to enhanced photocatalytic degradation of the dyes because of combined chemical and physical adsorption mechanisms. Toward the two rhodamine dyes, the TiO_2@MPS particles show significantly enhanced photocatalytic activity per TiO_2 than P25 under both UV and visible light irradiation. Especially under visible irradiation, the degradation rate constants of rhodamine B and rhodamine 6G molecules per TiO_2 were higher, 18 and 45 times, respectively, for the TiO_2@MPS particles than for P25. Toward methyl orange dye, the degradation rate constant per TiO_2 was lower for the TiO_2@MPS particles than for P25 under UV irradiation but it was eight times higher under visible irradiation. The TiO_2@MPS particles were recyclable and their photocatalytic activity did not change at all at least for three repeated photo-degradation tests.

Electronic supplementary material The online version of this article (doi:10.1007/s10853-015-8823-5) contains supplementary material, which is available to authorized users.

H. H. Yun · J. S. Kim · E. H. Kim · H. J. Lim · S. M. Koo
Department of Chemical Engineering, Hanyang University, Seoul 133-791, Korea
e-mail: yhh1217@hanmail.net

J. S. Kim
e-mail: icaruses@hotmail.com

E. H. Kim
e-mail: carrypotrick@gmail.com

H. J. Lim
e-mail: hyungjun.l@sukgyung.com

S. K. Lee · J. W. Kim · S. M. Koo (✉)
Department of Fuel Cells and Hydrogen Technology, Hanyang University, Seoul 133-791, Korea
e-mail: sangman@hanyang.ac.kr

S. K. Lee
e-mail: sangkyoung1225@gmail.com

J. W. Kim
e-mail: jinu404.kim@samsung.com

Introduction

Since the first report on photocatalytic reactivity of TiO_2 in 1972 [1], there has been a great deal of research on photocatalytic reactions due to their potential applications in environmental remediation and water decontamination through degradation of organic pollutants [2–8]. While various types of materials such as Bi_2O_3, ZnO, and CdS were studied, TiO_2 has been the most representative photocatalyst owing to its non-toxicity, chemical stability, low cost, and preferable band-gap energy. TiO_2 particles are

commercialized, for example P25 from Degussa Company, and currently utilized in industry. However, the photocatalyst TiO_2 suffers several limitations: First, its solar energy use efficiency is very low. Photocatalytic activity starts from electron excitation, followed by generation of radicals [7–9]. When light with enough energy—equal to or larger than the band gap energy of photocatalysts—is irradiated on the photocatalysts, their electrons in valence band are excited and electron–hole pairs are formed; with electron–hole separation, both electrons and holes make radicals degrade substances. The photocatalyst TiO_2 has a relatively large band gap of 3.2 eV (385 nm), requiring ultraviolet (UV) light to get excited directly to a conduction band for photocatalytic reactions. Because of the composition of sunlight (3 % UV, 44 % visible light, and the remainder infrared), solar energy use efficiency for the photocatalytic reactions by TiO_2 is very low. When colored dyes are attached or adjacent to photocatalysts, electrons can be generated from dyes and transferred to TiO_2. This process broadens the range of available light source to visible light but is less efficient than the direct excitation. Second, recombination of photo-generated electron–hole pairs often occurs, leading to early termination of the photo-catalytic reactions [9]. Moreover, commercial TiO_2 particles such as P25 have several weak points. P25 particles in aqueous suspension tend to form aggregates, reducing their photocatalytic efficiency; and it is not easy to collect P25 after use for recycling because of their nanometer size.

Various methods have been employed to improve the performance of TiO_2 to achieve higher photocatalytic efficiency, higher solar energy use efficiency (for instance, visible light excitable photocatalysts), and higher recyclability. Adopted methods so far include (1) changing the structure of TiO_2 [10, 11], for instance, exposing a high percentage of reactive facets so as to enhance its photocatalytic efficiency [12, 13]; (2) doping of TiO_2 with various metals and non-metals for elevation of photocatalytic activity via increasing electron mobility and inhibiting recombination of electron–hole pairs or for reducing the photonic band-gap to visible light region [14–19]; (3) composite formation of TiO_2 with various materials including silica, graphene, or activated carbon fiber for enhanced adsorption of target molecules [20–25]. Here, the photocatalytic degradation by short-lived reactive oxygen species becomes more efficient as target molecules and photocatalysts are in close proximity. Moreover, the photocatalytic activity of TiO_2 can also be enhanced by photosensitization of adsorbed target molecules—being excited by visible light and subsequently transferring electrons to the conduction band of the nearby TiO_2. Particularly, SiO_2 and TiO_2 composites have been developed in diverse types of structures such as core–shell TiO_2@SiO_2 materials and porous TiO_2/SiO_2 composites [26–33]. For instance, Chen et al. reported that the photocatalytic degradation efficiency of TiO_2/SiO_2 composite exhibited more than twice that of P25 and four times that of the synthesized TiO_2 particles when tested using rhodamine B under visible light irradiation [33]. They attributed these results to the facts that SiO_2 shifts the isoelectric point (IEP) of TiO_2 and therefore changes the surface charge of photocatalysts in experimental pH conditions, eventually altering the adsorption mode of dye molecules. For example, a negatively charged surface of photocatalysts would be preferred for adsorption of cationic dyes by inducing enhanced electrostatic interactions.

In this study, monodisperse, spherical 3-mercaptopropyl silica (MPS) particles of about 600 nm in diameter were prepared and coated with TiO_2 particles of a few nm in diameter to form core–shell-type TiO_2@MPS composite particles. The MPS particles were adopted in the composite-type photocatalyst design so as to enable chemical adsorption of target organic dyes, although they do not have photocatalytic activity. This would lead to enhanced adsorption and photocatalytic degradation of the dyes compared to previously reported TiO_2/SiO_2 photocatalysts because of combined chemical and physical adsorption mechanisms. It was considered that the proposed composite particles would show better recyclability than P25, due to their size. The TiO_2@MPS particles were tested for their photocatalytic activities under several different conditions—with variation of light sources (UV light and visible light) and reaction medium (different pHs and solvents). Three different organic dye molecules—rhodamine B, rhodamine 6G, and methyl orange, each having different degrees of chemical interaction with MPS particles—were selected for the tests. The TiO_2@MPS particles exhibited significantly enhanced adsorption characteristics and photocatalytic efficiency toward the organic dye molecules as well as superior recyclability, compared to commercial P25. The proposed composite particle design can comprise different types of chemical interactions by replacing MPS with organically modified silica particles containing other organic functional groups such as amine, epoxy, vinyl, isocynate.

Experimental

Materials

3-Mercaptopropyl trimethoxysilane, MPTMS, (97 wt%) was obtained from Sigma-Aldrich (St. Louis, USA) and titanium iso-propoxide ($Ti(OCH(CH_3)_2)_4$, 97 %) was obtained from Alfa Aesar (Ward Hill, USA). Ammonium hydroxide solution (NH_4OH, 30 wt% as NH_3), nitric acid (HNO_3, 60 wt%), ethanol, acetone, hexane, methanol, and

sodium hydroxide pellet were purchased from Daejung (Siheung, Korea). Titanium dioxide (AEROXIDE® TiO_2 P25) was obtained from Evonik Degussa (Essen, Germany).

Rhodamine B ($C_{28}H_{31}ClN_2O_3$) was obtained from Junsei Chemical Co., Ltd (Tokyo, Japan); methyl orange ($C_{14}H_{14}N_3NaO_3S$) was obtained from Showa Chemical Co., Ltd (Tokyo, Japan); and rhodamine 6G ($C_{28}H_{31}N_2O_3Cl$) was obtained from Sigma-Aldrich (St. Louis, USA).

Characterization methods

For particles' size and morphology, the samples were examined by transmission electron microscopy (TEM) using a JEM 2010 from JEOL (Japan), and by scanning electron microscopy (SEM) using Nova Nano SEM from FEI Corporate (USA). To calculate the TiO_2 contents on the particles, Inductively Coupled Plasma Atomic Emission Spectroscopy (ICP-AES) using OPTIMA 4300DV from Perkin-Elmer (USA) was used. The dye concentration was measured using UV/vis absorption spectrometer, S-4100 from Scinco Co., Ltd (Seoul, Korea). Zeta potential was measured by Zetasizer 3000 HAS from Malvern Instruments (UK).

Syntheses

MPS particles

Spherical MPS particles were prepared according to the previously reported method [34]. First, a 0.2-ml aliquot of HNO_3 was added into a round-bottomed flask containing 300 ml of de-ionized water at 70 °C. 4 ml (20.74 mol) of 3-mercaptopropyl trimethoxysilane (MPTMS) was added to the acid solution. After 2 min, a 20-ml aliquot of NH_4OH was added to the reaction mixture solution. The solution was kept stirred with a magnetic bar at 300 rpm for 4 h. The products were then washed with de-ionized water three times, filtered, and allowed to dry at 50 °C for 12 h.

TiO_2 nanosols

15 ml of $Ti(OiPr)_4$ was injected into a round-bottomed flask containing 250 ml of de-ionized water and the mixture was stirred at 300 rpm. After 10 min, 1.9 ml of HNO_3 was put into the mixture solution for peptization of precipitated solids. Then the solution was degassed and stirred at 60 °C for 6 h. The products were then dried at 50 °C for 12 h.

TiO_2@MPS particles

0.5 g of MPS particles was mixed with 50 ml of de-ionized water and sonicated for 1 h. The particle solution was then stirred at 300 rpm and a 1-ml aliquot of $Ti(OiPr)_4$ was added. After 30 min, a 0.5-ml aliquot of HNO_3 was injected into the solution. The solution was degassed and reacted at 70 °C for 4 h. The products were washed with de-ionized water three times, filtered, and then allowed to dry at 50 °C for 12 h.

Photo-degradation experiments

Photo-degradation experiments of three different organic dye molecules were carried out at ambient temperature in the presence of photocatalyst particles (TiO_2@MPS particles, P25, or TiO_2 nanosols) under visible or ultraviolet light irradiation so as to evaluate these particles' photocatalytic activities. First, mixtures of each photocatalyst and one of the three organic dyes were prepared in water as follows: A selected amount of each photocatalyst—0.1 g of TiO_2@MPS particles, 0.005 g TiO_2 nanosol, or 0.005 g of P25—were added into a 250-ml beaker containing 99 ml of de-ionized water, sonicated for 1 h, and stirred at a rate of 200 rpm with a magnetic bar. The beaker was tightly covered with plastic wrap to prevent evaporation of water. Then, a 1-ml aliquot of one of the three dye stock solutions, 1×10^{-3} M in water, was injected into the prepared dispersion of each photocatalyst to make 1×10^{-5} M dye in the photocatalyst dispersion. In case of TiO_2@MPS particles, a larger amount of the stock solutions were used for the two rhodamine dyes, in consideration of their high dye adsorption efficiency (See dye adsorption results below)—so as to make the free dye concentration in liquid phase of the dispersion at the beginning of the photo-degradation experiments to be approximately the same as those for P25 and TiO_2 nanosol. Note that in this study, the photo-degradation rates were measured by monitoring the dye concentrations in the liquid phase. Each dye-photocatalyst mixture solution was stirred for 30 min in a light-blocked chamber before light illumination started. For visible light degradation experiments, we used a home-built radiation chamber, $30 \times 30 \times 30$ (cm), which is blocked from outside light and has a visible light source, three-wavelength lamp of 100 W (EFHE 100EX-D) obtained from CityELG (Incheon, Korea), at the center of the ceiling. The beaker was located in the center of the radiation chamber and the distance between the lamp and the bottom of the beaker was set to be 20 cm. In case of UV light degradation experiments, a radiation chamber (RX-P12) containing a light source covering 300–420 nm with maximum intensity of 7.6 mW/cm^2 and power of 1 kW at 365 nm, from Raynics Co. (Gwangmyoung, Korea), was used. The distance between the light source at the ceiling and the bottom of the beaker was 13 cm. 1.5-ml aliquots of the dye-photocatalyst particle solution were sampled just before light irradiation as well as at every 20 or 60 min

after visible light irradiation and at every 1, 1.25 or 5 min after UV light irradiation. The collected sample solutions were then centrifuged for 5 min with 1.1×10^4 rpm in a micro-centrifuge so as to separate clear supernatant liquid and precipitated particles. The UV/vis absorption spectra of the liquid samples were then obtained to monitor the intensity change as well as the wavelength shift in the absorption peaks.

For TiO_2@MPS particles, effects of pH and solvent on the photo-degradation of rhodamine B under visible light irradiation were also studied by the same procedure as described above. The tested pH values were pH 3, 5, 7, and 9. The tested solvents include acetone and ethanol.

Dye adsorption and desorption experiments

Dye adsorption experiments were performed in the dark as control experiments for photo-degradation experiments. First, aqueous mixtures of dyes and photocatalysts were prepared for use in photo-degradation experiments. The mixture solutions were kept stirred in the dark. Sampling and analysis were performed as described for photo-degradation experiments to estimate the amount of dye adsorption on the photocatalysts. Dye desorption experiments were performed to select the solvent suitable for recyclability tests. The dye-loaded photocatalyst particles (TiO_2@MPS) were treated with various solvents and the amount of desorbed dye was measured. First, TiO_2@MPS particles containing a controlled amount of rhodamine B were prepared as follows: 0.1 g of TiO_2@MPS particles was dispersed in 100 ml of 1×10^{-5} M rhodamine B solution and let dye molecules adsorbed onto the particles for 36 h; the photocatalysts were then filtered and dried at 50 °C for 12 h. Second, the obtained rhodamine B loaded particles were weighed to make 50 ml of a 0.1 wt% colloidal solution in each of the solvents such as ethanol, methanol, acetone, and hexane. Each solution was then stirred at 200 rpm inside a light-blocked chamber during the whole desorption process so as to prevent the photo-degradation of the dye molecules. Third, 1.5-ml aliquots of the solution were sampled, first, at 12 h, and then every 24 h for 4 days. The sample solutions were centrifuged for 5 min with 1.1×10^4 rpm using the micro-centrifuge, and the UV/vis absorbance spectra of supernatant solutions were obtained to measure the amount of rhodamine B released from the particles.

Recyclability tests

Recyclability test was carried out for TiO_2@MPS particles by repeating photo-degradation experiments and recovery of the photocatalysts. For the photo-degradation experiments, 100 ml of 2×10^{-5} M rhodamine B aqueous solution and 0.1 g of the photocatalyst (new or recovered) were mixed and stirred for 30 min in the dark and then exposed to visible light irradiation for 4 h. 1.5-ml aliquots were sampled at every 60 min. For recovery of the photocatalysts, the photocatalyst particles in the mixture were collected, and washed thoroughly with the solvent selected through dye desorption tests so as to remove the adsorbed dyes. The particles were then dried at 50° C for 12 h so as to be used in the photo-degradation experiments.

Results and discussion

Physicochemical characterization of photocatalysts

Electron microscopic observations were performed for MPS particles, TiO_2 nanosols, and TiO_2@MPS particles as shown in Fig. 1. Figure 1a exhibits an SEM image of MPS particles, having smooth surfaces, with diameter of about 600 nm and Fig. 1b shows a TEM image of TiO_2 nanosols prepared by the peptization method. The syntheses and TiO_2 nano-particles coatings of MPS particles were found to be quite reproducible within an experimental error limit. Figure 1c exhibits TEM and SEM images of TiO_2@MPS particles, revealing that they maintain the spherical shape of MPS particles but their surfaces are rougher because of the surfaces being coated with tiny TiO_2 particles. It has been known that the important factor influencing photocatalytic activity of the TiO_2@MPS particles is the total surface area of TiO_2 particles as well as the amount of TiO_2. From ICP-AES result, the TiO_2 content in TiO_2@MPS was found to be 1.6 % (w/w), which indicated very thin layers of TiO_2 coating on MPS particles. Therefore, we assumed that most of TiO_2 particles were located evenly on the surface of MPS particles and TiO_2 layer thickness would not influence photocatalytic activity of the TiO_2@MPS particles.

The isoelectric point (IEP) of TiO_2@MPS particles—the pH where particle surface carries no net electrical charge, i.e., the zeta potential becomes zero—was determined by measuring zeta potentials at different pHs. The IEP measurements were also performed for P25 (AEROXIDE® TiO_2), a commercial photocatalyst that is prepared by vapor-phase process, and TiO_2 nanosols for comparison. It is known that in an aqueous solution, for pH lower than IEP, the surface charge of the suspended particles is positive, whereas for pH higher than IEP, the surface charge is negative. The zeta potential data show that IEP of TiO_2@MPS particles is lower than pH 2.5, while the IEP of TiO_2 nanosol is around pH 3–4. The IEP of P25 is around pH 6 (Fig. S1). The IEP difference between P25 and TiO_2 nanosol, despite the same composition (TiO_2), may result

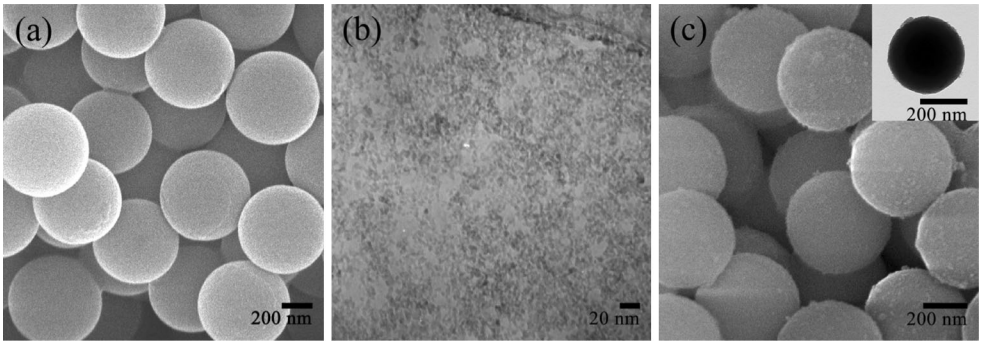

Fig. 1 SEM image of particles (**a**), TEM image of TiO_2 nanosol (**b**), and SEM and TEM image of TiO_2@MPS particles (**c**)

from difference in production processes, i.e., solution phase versus gas phase.

Dye adsorption characteristics of photocatalysts

The focus of this study is the enhancement in photo-catalytic activity through the chemical interaction between chemically modified substrate particles and organic dye molecules. The MPS particles were adopted in the composite-type photocatalyst design so as to enable chemical adsorption of target organic dyes, although they do not have photocatalytic activity. As a proof of evidence, dye adsorption capabilities of two photocatalysts, TiO_2@MPS and P25, were investigated using rhodamine B, rhodamine 6G, and methyl orange dyes. The free dye concentration in solution dropped immediately after mixing with photocatalysts but subsequent reduction of the dye concentration was relatively negligible for both catalysts, indicating that dye adsorption on the photocatalysts is a fast process (Fig. S2). For TiO_2@MPS, the amounts of initial adsorption of organic dyes are 43 % for rhodamine 6G, 35 % for rhodamine B, and 18 % for methyl orange. For P25, the initial dye adsorption amounts were 1 % for rhodamine 6G, 6 % for rhodamine B, and 30 % for methyl orange, respectively. Such difference in the dye adsorption characteristics of the two photocatalysts may be related with available functional groups and surface charges of the photocatalysts and the dyes. This would lead to enhanced photocatalytic degradation of the dyes compared to previously reported photocatalysts because of combined chemical and physical adsorption mechanisms. As MPS particles have acidic SH groups, dyes containing basic functional groups such as amine can be preferentially adsorbed on them by ion pair interactions. Moreover, zeta potential measurements showed that in an acidic solution (for pH 3–6), TiO_2@MPS particles have negative surface charges but P25 particles have positive surface charges. It is expected that dyes would be preferentially adsorbed to the photocatalysts by electrostatic interaction if the dyes have opposite charges to those of the photocatalysts, i.e., positively charged dyes to TiO_2@MPS and negatively charged dyes to P25. The chemical structures of the dyes indicate that the observed adsorption trends for the two photocatalysts above are well matched with such expectations. Rhodamine B and rhodamine 6G have similar chemical structures—containing two amine groups but rhodamine B contains a carboxyl group while rhodamine 6G has an ester group instead—resulting in higher positive charges for rhodamine 6G than for rhodamine B (Fig. S3). On the other hand, methyl orange is an anionic dye with a sulfonate group, which exhibits better adsorption behavior toward P25 than TiO_2@MPS particles.

Photo-catalytic activities of TiO_2@MPS particles, P25, and TiO_2 nanosols

Photo-degradation of rhodamine B, rhodamine 6G, and methyl orange in the presence of TiO_2@MPS, P25, or TiO_2 nanosol particles were investigated under UV or visible light irradiation. For the photocatalytic activity test, the most of previous studies, including references cited in our manuscript, exhibited the results with a single measurement for photo-catalytic activity at each specific condition, without presenting averages or error bars. It was found that the most of photocatalytic degradation studies of organic dyes were carried within a given set of reaction conditions and the results of self-sustaining trends, not absolute data values, were analyzed by the researchers. We had also investigated the reproducibility of photocatalytic activity for rhodamine B dye under visible irradiation and obtained good reproducible data (Fig. S4). Figure 2 shows the UV/vis spectra of rhodamine B obtained at different time points during the photo-degradation experiments. We note that spectral changes during UV irradiation include only the decrease in the dye's absorption peak intensity as shown in Fig. 2a, b. However, those during visible irradiation include not only the peak intensity reduction but also the peak wavelength shift toward blue. We also note that the

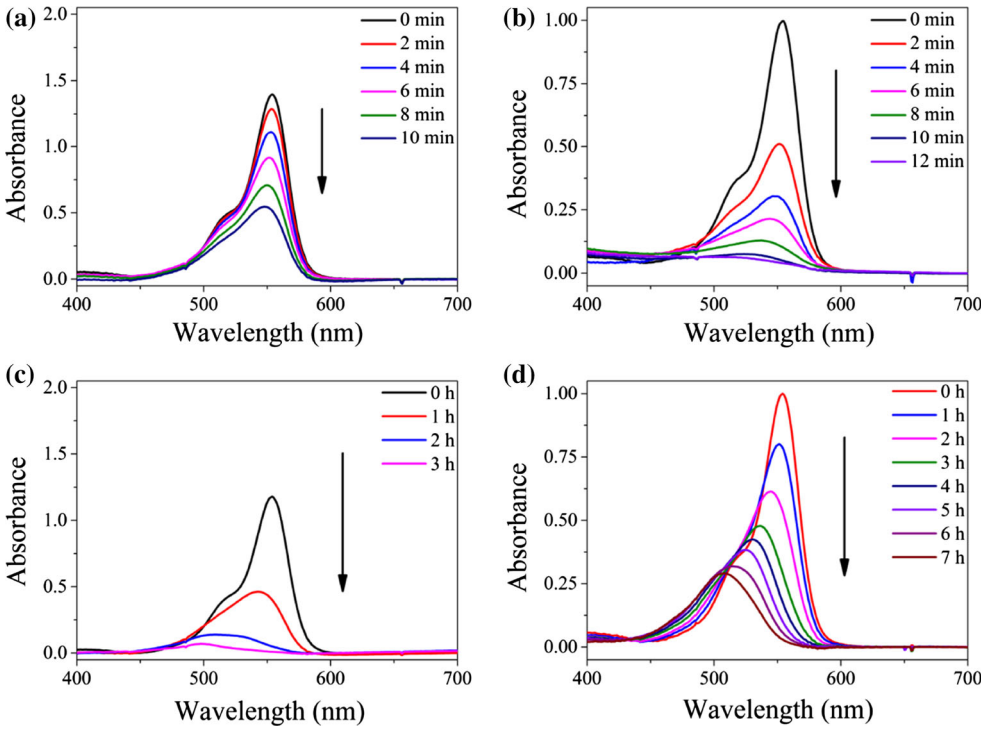

Fig. 2 UV/vis spectra of rhodamine B during photocatalytic degradation: Under UV light irradiation, with TiO_2@MPS (**a**), and with P25 (**b**); under visible light irradiation, with TiO_2@MPS (**c**) and with P25 (**d**)

rhodamine B degraded much faster under UV irradiation than under visible irradiation for both TiO_2@MPS and P25. These observations indicate different photo-degradation mechanisms for UV and visible light. So far, there are two proposed mechanisms to explain the photocatalytic degradation of dye molecules: Photocatalytic oxidation and photosensitized oxidation [8].

The photocatalytic oxidation involves direct photo-excitation of an electron in the valence band (VB) of TiO_2 into the conduction band (CB) and is the dominant mechanism for dye degradation by UV irradiation. Here, the dye chromophore is directly cleaved by reactive oxygen species (ROS), leading to immediate destruction of the dye molecule. The photosensitized oxidation is initiated by photo-excitation of an electron in the VB of dyes, followed by transferring the electron to the CB of TiO_2. Degradation under visible light can be explained by this mechanism. It should be noted that the electron transfer from dye to TiO_2 is efficient only if the dyes are located in close proximity of TiO_2. Therefore, it is expected that dye adsorption on photocatalysts would play an important role for degradation of dyes under visible light, as the adsorbed dyes would be close to TiO_2. Figure 2c, d confirm it by showing that degradation of rhodamine B by TiO_2@MPS is notably faster than by P25, under visible irradiation. Note that rhodamine B can be adsorbed on TiO_2@MPS much more efficiently than on P25—by factor of $\sim$6 under current experimental conditions according to the dye adsorption results. Moreover, since dye adsorption on the photocatalysts is a limiting factor for photosensitized oxidation to occur, photo-degradation of dyes under visible irradiation would be slower than under UV irradiation as we observed here. The observed peak shift during visible irradiation indicates that the decomposition pathway of rhodamine B involves de-ethylation of diethyl amino group, followed by destruction of chromophore structure, rather than direct chromophore cleavage [35–37].

For quantitative comparison of photocatalytic activities of the three photocatalysts, the evolution of the absorption peak intensity of rhodamine B as a function of irradiation time is plotted for each of the three photocatalysts. Under UV light irradiation, P25 degraded rhodamine B the fastest, followed by TiO_2@MPS particles and then TiO_2 nanosol the slowest, according to Fig. 3a. The rhodamine B degradation reactions followed the first-order kinetics and the degradation rate constants were 0.22, 0.17, and 0.11 min^{-1} for P25, TiO_2@MPS, and TiO_2 nanosol, respectively (Fig. S5). However, under visible light irradiation, TiO_2@MPS particles exhibited the fastest degradation rate, followed by P25 and then TiO_2 nanosol (Fig. 3b). It could be observed that P25 still exhibited observable photocatalytic activity under visible irradiation. This phenomenon can be explained as follows: For P25, dye degradation usually occurs through both photocatalytic oxidation and photosensitized oxidation processes. Under visible light irradiation, a photosensitized oxidation path allows pure P25 to degrade dye molecules over 50 % after 400 min, although photodegradation under UV light irradiation was more

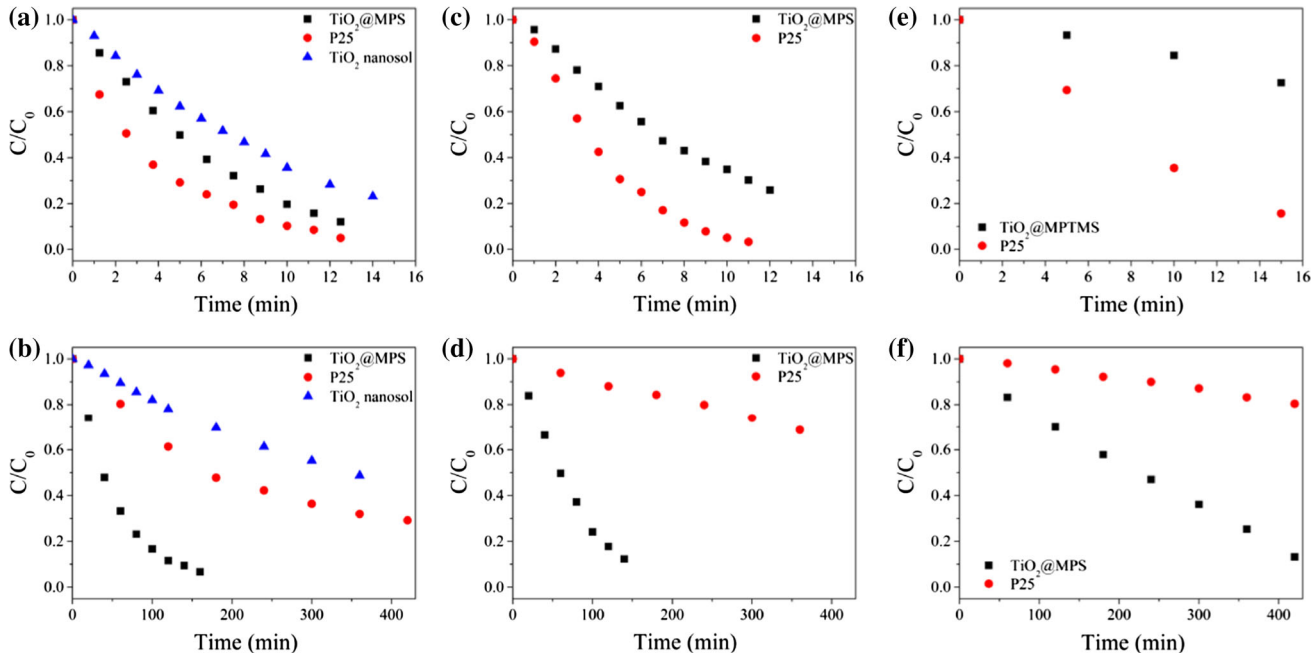

Fig. 3 Comparison of photocatalytic activity of TiO_2@MPS, P25, and TiO_2 nanosol under UV light irradiation (*top*) and visible light irradiation (*bottom*). Rhodamine B dye degradation (**a**, **b**); rhodamine 6G degradation (**c**, **d**); methyl orange degradation (**e**, **f**)

complete and much faster compared to degradation under visible light. Our previous studies also indicated that more than 50 % of rhodamine B was degraded under visible light irradiation using P25 after longer than 3 h [38].

The rate constants by the TiO_2@MPS particles, P25, and TiO_2 nanosol were 0.017, 0.003, and 0.002 min^{-1}, respectively. It should be pointed out that in these photo-degradation experiments, the TiO_2 amount included in the TiO_2@MPS particles is only about 1/3 of the amount of P25 and TiO_2 nanosol, considering the TiO_2 content per TiO_2@MPS particles (1.6 % by ICP-AES). Therefore, the rate constant per g of TiO_2 by the TiO_2@MPS particles is greater than those of TiO_2 nanosol and P25 by a factor of 26 and 18, respectively, under visible irradiation. In case of UV irradiation, the rhodamine B degradation rate constant by TiO_2@MPS particles is two and four times higher than those of P25 and TiO_2 nanosol, respectively. The ultra-high photocatalytic efficiency of the TiO_2@MPS particles under visible light irradiation is believed to be mostly due to a large amount of rhodamine B molecules being adsorbed on the TiO_2@MPS particles through physical and chemical interactions, enabling highly enhanced electron transfer from the dyes to TiO_2, compared to P25 and TiO_2 nanosol. The TiO_2@MPS particles are also better photocatalysts toward rhodamine B than P25 under UV light irradiation, unlike previous report with TiO_2/SiO_2 composite photocatalysts which showed lower UV-degradation efficiency but higher visible-degradation efficiency than P25 [33]. This suggests that photo-degradation of dyes under UV irradiation may also be affected by dye adsorption as photocatalysts with higher adsorption efficiency may have more dye molecules near them and therefore degrade the dye molecules more efficiently. Another reason for the better photocatalytic efficiency of TiO_2@MPS particles than TiO_2 nanosol and P25 under UV irradiation may be their structure that prevents aggregation of TiO_2 nanoparticles (See Fig. 1c). Note that aggregation of TiO_2 nanoparticles is a notorious problem that causes reduction of their photo-degradation efficiency over time. These results demonstrate the important role of MPS particles in the design of the core–shell-type photocatalyst particles. It is interesting to observe that P25 shows better photocatalytic efficiency toward rhodamine B than TiO_2 nanosol under both UV and visible irradiation, although both particles are TiO_2 particles of a few nanometers in size. This may result from P25 having better crystallinity than TiO_2 nanosol as the photo-degradation rates are known to be affected by crystallinity of TiO_2 particles [38].

Figure 3c, f shows the results on photocatalytic degradation of other colored organic dyes, rhodamine 6G and methyl orange in the presence of TiO_2@MPS particles and P25 under UV and visible light irradiation. The kinetic studies suggested that rhodamine 6G and methyl orange are also degraded following first-order equation like rhodamine B (Fig. S5). The rate constants for degradation of rhodamine 6G by TiO_2@MPS particles and P25 were 0.11 and 0.31 min^{-1}, respectively, under UV light irradiation, while they were 0.015 and 0.001 min^{-1} under visible light

irradiation. The rate constants for degradation of methyl orange by TiO_2@MPS particles and P25 were 0.02 and 0.12 min^{-1}, respectively, under UV irradiation, while they were 0.004 and 0.0005 min^{-1}, respectively, under visible irradiation. According to the kinetic analysis per g of TiO_2, TiO_2@MPS particles showed higher photocatalytic efficiency toward rhodamine 6G than P25—slightly higher under UV irradiation and significantly higher under visible irradiation, which is the same trend as observed for photo-degradation of rhodamine B. Especially for rhodamine 6G degradation under visible light irradiation, the degradation rate constant per TiO_2 by TiO_2@MPS particles was ~45 times that by P25, which confirms that dye adsorption is a dominant factor for visible light degradation of dyes. However, in case of degradation of methyl orange, the degradation rate constant per TiO_2 by TiO_2@MPS particles is slightly lower than P25 under UV irradiation, but higher than that by P25 by a factor of ~8 under visible light irradiation, despite that they show lower methyl orange adsorption efficiency than P25. We also note that the methyl orange degradation rate is notably lower than those for the two rhodamine dyes under both UV and visible irradiation. This may be due to the chemical structure of methyl orange—it does not contain ethyl groups so there is no deethylation pathway during photo-degradation unlike the rhodamine dyes. All these photo-degradation study results demonstrate that TiO_2@MPS particles have significantly enhanced photocatalytic efficiency and solar energy use efficiency compared to P25.

pH and solvent effects on photocatalytic activities of TiO_2@MPS particles

Photocatalytic degradation can be affected by pH and solvent of reaction medium. For studying the pH effect, degradation experiments of rhodamine B in aqueous solutions, of various pHs, containing TiO_2@MPS under visible light irradiation were carried out, as shown in Fig. 4. The rate of photocatalytic degradation increased as pH of solution decreased—the rate constant was five times higher at pH 3 than at pH 7. With pH of 9, almost no degradation of rhodamine B dyes occurred. These results may be explained by pH-dependent dye adsorption characteristics of the particles as pH affects both the surface charge of photocatalyst particles and the charge of dye molecules. Under acidic condition, TiO_2@MPS catalyst particles have negatively charged surface and dye molecules become more positive, increasing electrostatic interaction. More of the dyes can be adjacent to TiO_2 due to enhanced adsorption of the dyes onto the photocatalysts, which will facilitate the electron transfer from the dyes to conduction band of TiO_2. It will also facilitate the degradation of the dyes by generated OH radicals as the action of OH radical

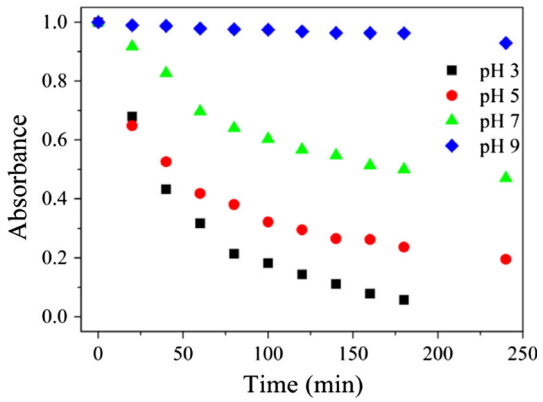

Fig. 4 pH dependence on degradation of rhodamine B using TiO_2@MPS under visible light irradiation

is very localized due to its very short lifetime (~ns) [39]. Consequently, the photosensitized degradation efficiency of the TiO_2@MPS particles becomes high in acidic solutions. However, at pH 9, both rhodamine B and the TiO_2@MPS particles are negatively charged, resulting in almost no adsorption of rhodamine B on the particles and hence no photosensitized oxidation of the dyes. It was found that there was negligible pH changes during the organic dyes degradation, which would not influence the generation of *OH radicals (Table S1).

For studying the solvent effect, photocatalytic degradation of rhodamine B in acetone and ethanol containing P25 or TiO_2@MPS particles was investigated under visible light irradiation. Both P25 and TiO_2@MPS particles decomposed rhodamine B dyes completely in acetone within less than an hour—significantly faster degradation of the dyes than in water—but there was no detectable decomposition of the dye molecules in ethanol (Fig. S6). This is due to the fact that production and stability of ROS such as OH radical and O_2^- (superoxide anion)—that are believed to play a dominant role for photocatalytic degradation of organic dyes—are affected by solvents. In protic solvents such as ethanol and acetic acid, OH radicals are quickly scavenged, while aprotic solvent like acetone, there will be no such radical scavenge effect [40, 41]. Note that water is a weak protic solvent. Resultantly, ROS have longer lifetime in acetone than in ethanol or in water, resulting in enhanced photo-catalytic degradation efficiency in acetone. Moreover, the solubility of oxygen molecules is higher in acetone than in water, and the higher O_2 concentration in solution leads to generation of higher amount of ROS [42].

Recyclability of TiO_2@MPS particles

For practical applications, it would be cost-effective if photocatalysts could be used several times without

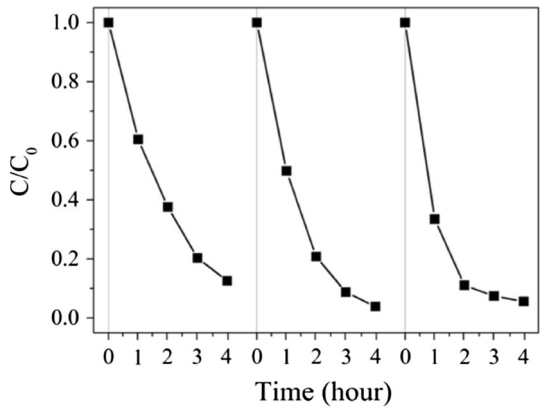

Fig. 5 Recyclability of TiO_2@MPS for rhodamine B photo-degradation

significantly losing their catalytic activities. The recyclability of the TiO_2@MPS particles was investigated by repeating photo-degradation experiments using the same particles, first fresh ones and then recovered ones. For recovery of the particles, dye desorption process was performed followed by drying process. First, desorption experiments of organic dye molecules from recycled catalysts were carried out using various types of solvents so as to select the proper solvent for the recovery process. When polar protic solvents—methanol, and ethanol—were used, rhodamine B dye came out to solvent easily with 24 h stirring, while polar aprotic solvents such as acetone could not desorb dye molecules as much as polar protic solvents did. On the other hand, non-polar solvents like hexane did not make the dye molecules be released from the catalysts at all. Based on these results, ethanol was selected as the solvent for dye desorption experiments. As can be seen in Fig. 5, the photocatalytic degradation efficiency of TiO_2@MPS particles toward rhodamine B remained almost the same even at the third time use. We also note that the morphology of recycled catalysts remained the same.

Conclusions

Core–shell-type TiO_2@MPS particles were designed to have enhanced dye adsorption capability through both chemical and physical adsorption mechanisms, and thereby to show enhanced photocatalytic activity toward target organic dyes. Here, MPS particles were employed to serve the following functions: (1) to hold the TiO_2 on their surface; (2) to provide the chemical interaction between dyes and available organic functional groups of the particles. Photocatalytic activity of the TiO_2@MPS particles under visible light irradiation was 18, 45, and 8 times better than P25 toward rhodamine B, rhodamine 6G, and methyl orange dye molecules, respectively, based on the measured first-order rate constants per TiO_2. The recyclability of the TiO_2@MPS particles was investigated to find that the photocatalytic activity did not change at all even for the third time use in the photo-degradation experiments. This demonstrates that the TiO_2@MPS particles have markedly enhanced photocatalytic efficiency toward organic dye molecules as well as excellent recyclability, compared to commercial P25. It is expected that by replacing the MPS particles with other organically modified silica particles containing different chemical functional groups, the adsorption characteristics of the core–shell-type photocatalysts toward desired organic molecules can be controlled.

Acknowledgements This work was supported by the Human Resources Development Program (NO. 20094020200010) of the Korea Institute of Energy Technology Evaluation and Planning (KETEP) grant funded by the Korea government Ministry of Trade, Industry and Energy and also supported by Nano-Convergence Foundation (www.nanotech2020.org) funded by the Ministry of Science, ICT and Future Planning (MSIP, Korea) & the Ministry of Trade, Industry and Energy(MOTIE, Korea) (Project Name: 1415131476) and Hanyang Science and Technology Scholarship Program.

References

1. Fujishima A, Honda K (1972) Electrochemical photolysis of water at a semiconductor electrode. Nature 238:37–38
2. Kabra K, Chaudhary R, Sawhney RL (2004) Treatment of hazardous organic and inorganic compounds through aqueous-phase photocatalysis: a review. Ind Eng Chem Res 43:7683–7696
3. Malato S, Fernández-Ibáñez P, Maldonado MI, Blanco J, Gernjak W (2009) Decontamination and disinfection of water by solar photocatalysis: recent overview and trends. Catal Today 147:1–59
4. Gaya UI, Abdullah AH (2008) Heterogeneous photocatalytic degradation of organic contaminants over titanium dioxide: a review of fundamentals, progress and problems. J Photochem Photobiol C 9:1–12
5. Linsebigler AL, Lu G, Yates JT (1995) Photocatalysis on TiO_2 surfaces: principes, mechanisms, and selected results. Chem Rev 95:735–758
6. Nakata K, Fujishima A (2012) TiO_2 photocatalysis: design and applications. J Photochem Photobiol C 13:169–189
7. Pelaez M, Nolan NT, Pillai SC et al (2012) A review on the visible light active titanium dioxide photocatalysts for environmental applications. Appl Catal B 125:331–349
8. Konstantinou IK, Albanis TA (2004) TiO_2-assisted photocatalytic degradation of azo dyes in aqueous solution: kinetic and mechanistic investigations a review. Appl Catal B 49:1–14
9. Turchi CS, Ollis DF (1990) Photocatalytic degradation of organic water contaminants: mechanisms involving hydroxyl radical attack. J Catal 122:178–192
10. Chen LH, Li XY, Deng Z et al (2013) Hydrothermal and surfactant treatment to enhance the photocatalytic activity of hierarchically meso-macroporous titanias. Catal Today 212:89–97

11. Kao LH, Hsu TC, Lu HY (2007) Sol–gel synthesis and morphological control of nanocrystalline TiO_2 via urea treatment. J Colloid Interface Sci 316:160–167
12. Ong WJ, Tan LL, Chai SP, Yong ST, Mohamed AR (2014) Facet-dependent photocatalytic properties of TiO_2-based composites for energy conversion and environmental remediation. ChemSusChem 7:690–719
13. Han X, Kuang Q, Jun M, Xie Z, Zheng L (2009) Synthesis of titania nanosheets with a high percentage of exposed (001) facets and related photocatalytic properties. J Am Chem Soc 131:3152–3153
14. Pang YL, Abdullah AZ (2013) Effect of carbon and nitrogen co-doping on characteristics and sonocatalytic activity of TiO_2 nanotues catalyst for degradation of rhodamine B in water. Chem Eng J 214:129–138
15. Ohno T, Akiyoshi M, Umebayashi T, Asai K, Mitsui T, Matsumura M (2004) Preparation of S-doped TiO_2 photocatalysts and their photocatalytic activites under visible light. Appl Catal A 265:115–121
16. Umebayashi T, Yamaki T, Tanaka S, Asai K (2003) Visible light-induced degradation of methylene blue on S-doped TiO_2. Chem Lett 32:330–331
17. RA, Morikawa T, Ohwaki T, Aoki K, Taga Y (2001) Visible-light photocatalysis in nitrogen-doped titanium oxides. Science 293:269–271
18. Cong Y, Zhang K, Chen F, Anpo M (2007) Synthesis and characterization of nitrogen-doped TiO_2 nanophotocatalyst with high visible light activity. J Phys Chem C 111:6976–6982
19. Mahlambi MM, Mishra AK, Mishra SB, Krause RW, Mamba BB, Raichur AM (2013) Metal doped nanosized titania used for the photocatalytic degradation of rhodamine B dye under visible-light. J Nanosci Nanotechnol 13:4934–4942
20. Fukugaichi S, Henmi T, Matsue N (2013) Facile synthesis of TiO_2-zeolite composite and its enhanced photocatalytic activity. Catal Lett 143:1255–1259
21. Liu H, Dong X, Wang X, Sun C, Li J, Zhu Z (2013) A green and direct synthesis of graphene oxide encapsulated TiO_2 core/shell structures with enhanced photoactivity. Chem Eng J 230:279–285
22. Zhang H, Lv X, Li Y, Wang Y, Li J (2010) P25-graphene composite as a high performance photocatalyst. ACS Nano 4:380–386
23. Muthirulan P, Devi CN, Sundaram MM (2014) TiO_2 wrapped graphene as a high performance photocatalyst for acid orange 7 dye degradation uner solar/UV light irradiations. Ceram Int 40:5945–5957
24. Meng H, Hou W, Xu X, Xu J, Zhang X (2014) TiO_2-loaded activated carbon fiber: hydrothermal snythesis, adsorption properties and photocatalytic activity under visible light irradation. Particuology 14:38–43
25. Zhou W, Pan K, Qu Y et al (2010) Photodegradation of organic contamination in wastewaters by bonding TiO_2/single-walled carbon nanotube composites with enhanced photocatalytic activity. Chemosphere 81:555–561
26. Lim SH, Phonthammachai N, White SSPTJ (2008) Simple route to monodispersed silica–titania core–shell photocatalysts. Langmuir 24:6226–6231
27. Hu JL, Qian HS, Li JJ, Hu Y, Li ZQ, Yu SH (2013) Synthesis of mesoporous SiO_2@TiO_2 core–shell nanospheres with enhanced photocatalytic properties. Part Part Syst Charact 30:306–310
28. Kim SK, Chang H, Cho K et al (2011) Enhanced photocatalytic property of nanoporous TiO_2/SiO_2 microparticles prepared by aerosol assisted co-assembly of nanoparticles. Mater Lett 65:3330–3332
29. Anderson C, Bard AJ (1995) An improved photocatalyst of TiO_2/SiO_2 prepared by a sol–gel synthesis. J Phys Chem 99:9882–9885
30. Lee JW, Othman MR, Eom Y, Lee TG, Kim WS, Kim J (2008) The effects of sonification and TiO_2 deposition on the micro-characteristrics of the thermally treated SiO_2/TiO_2 spherical core-shell particles for photo-catalysis of methyl orange. Microporous Mesoporous Mater 116:561–568
31. Xu J, Xiao X, Stepanov AL et al (2013) Efficiency enhancements in Ag nanoparticles-SiO_2-TiO_2 sandwiched structure via plasmonic effect-enhanced light capturing. Nanoscale Res Lett 8:73
32. Zhang X, Zhu Y, Yang X et al (2013) Enhanced visible light photocatalytic activity of interlayer-isolatedd triplex Ag@SiO_2@TiO_2 core–shell nanoparticles. Nanoscale 5:3359–3366
33. Chen F, Zhao J, Hidaka H (2003) Highly selective deethylation of rhodamine B: adsorption and photooxidation pathways of the dye on the TiO_2/SiO_2 composite photocatalyst. Int J Photoenergy 5:209–217
34. Kim JS, Kim SJ, Jung EG, Yun HH, Koo SM (2013) The preparation of titania nano crystals and silica–titania core–shell particles through peptization process. J Ceram Process Res 14:327–331
35. Wu T, Liu G, Zhao J, Hidaka H, Serpone N (1998) Photoassisted degradation of dye pollutants. V. Self-photosensitized oxidative transformation of rhodamine B under visible light irradiation in aqueous TiO_2 dispersions. J Phys Chem B 102:5848–5851
36. Yu K, Yang S, He H, Sun C, Gu C, Ju Y (2009) Visible light-driven photocatalytic degradation of rhodamine B over $NaBiO_3$: pathways and mechanism. J Phys Chem A 113:10024–10032
37. Wang Q, Chen C, Zhao D, Ma W, Zhao J (2008) Change of adsorption modes of dyes on fluorinated TIO_2 and its effect on photocatalytic degradation of dyes under visible irradiation. Langmuir 24:7338–7345
38. Sung-Suh HM, Choi JR, Hah HJ, Koo SM, Bae YC (2004) Comparison of Ag deposition effects on the photocatalytic activity of nanoparticulate TiO_2 under visible and UV light irradiation. J Photochem Photobiol A 163:37–44
39. Lubec G (1996) The hydroxyl radical: from chemistry to human disease. J Investig Med 44:324–346
40. Khodja AA, Sehili T, Pilichowski J-F, Boule P (2001) Photocatalytic degradation of 2-phenylphenol on TiO_2 and ZnO in aqueous suspensions. J Photochem Photobiol A 141:231–239
41. Daneshvar N, Salari D, Khataee AR (2003) Photocatalytic degradation of azo dye acid red 14 in water: investigation of the effect of operational parameters. J Photochem Photobiol, A 157:111–116
42. Battino R, Rettich TR, Tominaga T (1983) The solubility of oxygen and ozone in liquids. J Phys Chem Ref Data 12:163–178